Low volume, large force (>1mN) and nanometer resolution, electrostatic microactuator for low displacement applications

E. Sarajlic, E. Berenschot, G. Krijnen, M. Elwenspoek

Transducer Science Technology Group, MESA+ Research Institute,University of Twente
P.O. Box 217, 7500 AE Enschede, The Netherlands, *e.sarajlic@el.utwente.nl*

ABSTRACT

A compact electrostatic microactuator suitable for low displacement applications is proposed. The actuator employs a large number of basic units working in parallel together with a built-in mechanical transformation to generate large force. Influence of distinct design parameters on actuator performance was investigated. The actuator is successfully fabricated using the trench isolation technology. Displacement and generated force of the fabricated actuators, operated at pull-in, are measured using integrated springs and strain gauges. A large force (>1mN) with a controllable nanometer resolution step (<15 nm) was measured for a typical actuator design. The actuator fits in a volume of 200 x 62 x 5 μm and is operated by a voltage of 70 V. Characteristic applications can include the contraction/elongation body of an inchworm motor, vibration excitation or friction measurements.

Keywords: Electrostatic actuators, trench isolation

1 INTRODUCTION

Micromotors based on the inchworm motion [1-4] can provide a large displacement by adding small steps in sequence. Inchworm motors usually employ low displacement actuators, such as piezoelectric [1-2] or electrostatic gap-closing actuators [3], to generate a single step. N.Tas [4] proposed a promising approach for an alternative step generation (see Figure 1a). The electrostatic force generated by an applied voltage difference between an elastic plate and the substrate causes a lateral deflection of the plate. The lateral deflection of the plate towards the substrate induces a small but powerful contraction Δ due to a built-in mechanical transformation. This actuation principle is successfully implemented for step generation in an electrostatic shuffle motor [4] and for the friction measurement in micromachining [5].

In this paper a novel low displacement electrostatic microactuator, also based on the built-in mechanical transformation, is presented. The characteristics of the actuator in terms of operation voltage, maximum force and maximum displacement are investigated using mathematical models. The obtained closed-form expressions provide insight in the behavior of the actuator and influence of different design variables on the actuator performance. Various prototypes of the actuator are successfully fabricated and measurements of force and displacement are performed.

2 PRINCIPLE OF OPERATION

Figure 1b shows the principle of operation of the novel actuator. A basic cell of the actuator consists of two parallel conducting beams (plates). The beams are mechanically interconnected but electrically separated allowing individual biasing of each beam. On application of a potential difference an attractive electrostatic force occurs causing a deflection of the beams. The in-plane deflection induces a longitudinal displacement δ moving the ends of the beam closer together.

Using two beams (plates), with in-plane deflection, instead of a single one deflected towards the substrate yields additional benefits. First, unwanted rotation moment and normal force at the supporting ends are eliminated due to the symmetry. Furthermore, no substrate electrode is necessary for actuation giving larger design freedom for an eventual application in an inchworm motor. Finally, the actuator has a very interesting scalability as the number of basic cells operating in parallel can be chosen freely by design to increase generated force.

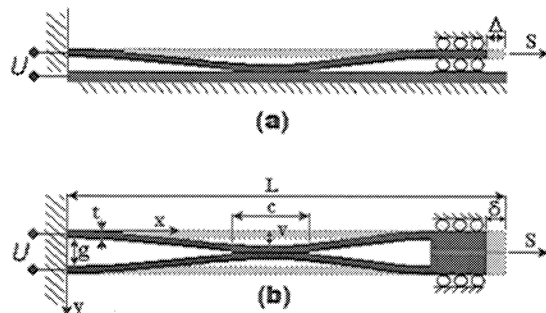

Figure 1: Electrostatic attractive force due to the applied voltage deflect the plate(s) causing a powerful contraction: (a) single plate actuator realized by N. Tas [4]; (b) a basic cell of the novel actuator consisting of two parallel beams (plates) mechanically connected and electrically isolated.

3 DESIGN

3.1 Pull-in voltage

An important design parameter for the proposed actuator is the pull-in voltage, the upper voltage limit beyond which the electrostatic attraction force between beams increases faster than the restoring elastic force causing instability and ultimately contact of the beams. In general, the pull-in voltage for a parallel plate capacitor with two movable electrodes U_{PI}^{II} can be expressed as:

$$U_{PI}^{II} = \frac{1}{\sqrt{2}} U_{PI}^{I} \quad (1)$$

where U_{PI}^{I} is the pull-in voltage of a capacitor with one movable and one fixed electrode. Hence, a first approximation of the pull-in voltage for two parallel double-clamped beams can be found using the expression for the pull-in voltage of single beam given in [6]:

$$U_{PI}^{II} = \frac{1}{\sqrt{2}} \sqrt{C_1 \frac{Et^3 g^3}{\varepsilon_0 L^4}} \quad (2)$$

where C_1=11.9 for a double-clamped beam [6], E is Young's modulus, t is the beam width, g is the mutual distance between the beams, L is the beam length and ε_0 is permittivity. For a proper operation of the actuator pull down of the actuator beams to the grounded substrate has to be avoided. By comparing the pull-in voltage to the substrate $U_{PI->S}^{I}$ with the lateral pull-in U_{PI}^{II}

$$\frac{U_{PI->S}^{I}}{U_{PI}^{II}} = \sqrt{\frac{C_1 \frac{Eh^3 d^3}{\varepsilon_0 L^4}}{\frac{C_1}{2} \frac{Et^3 g^3}{\varepsilon_0 L^4}}} = \sqrt{2} \frac{\left(\frac{h}{t}\right)^{\frac{3}{2}}}{\left(\frac{g}{d}\right)^{\frac{3}{2}}} \quad (3)$$

can be concluded that for the high aspect ratio beams (large h/t) a small gap d between the actuator and the substrate can be chosen. It is interesting to note that an actuator operated at lateral pull-in, with a mutual distance between beams g=2µm and the aspect ratio h/t=20 (achievable using DRIE process) allows suspension of the actuator above the grounded substrate on distance even smaller than 100 nm without pull down.

3.2 Maximum displacement

Due to bending the beams undergo a longitudinal deflection moving the ends of the actuator closer together. The displacement δ, called the curvature shortening, can be approximated as the difference between the length of a deflected beam and its horizontal projection [7], given by:

$$\delta = \frac{1}{2} \int_0^L \left(\frac{dy}{dx}\right)^2 dx \quad (4)$$

A reasonable approximation of the beam deflection curve is given by the following function, which satisfies the boundary conditions:

$$y(x) = \frac{1}{2} v (1 - \cos(\frac{2\pi x}{L})) \quad (5)$$

v is the beam deflection at the midpoint. The longitudinal displacement of an actuator operating in the stable regime, bellow the pull-in voltage, is obtained by substituting the assumed deflection profile in expression (4):

$$\delta = \frac{\pi^2}{4} \frac{v^2}{L} \quad (6)$$

When the actuation voltage exceeds the lateral pull-in voltage the actuator beams will make physical contact. In that case the lateral displacement is given by:

$$\delta = \frac{\pi^2}{16} \frac{g^2}{L} \frac{1}{1 - \frac{c}{L}} \quad (7)$$

where c is the length of the contact area. For a realistic actuator operated at the pull-in with g=2µm, L=200µm, c/L=0.2 (20% of the beam length in contact) is the longitudinal displacement in the nanometer range δ=15.4 nm.

3.3 Maximum force

The maximum force generated by the actuator, equals the force required to elongate a beam by the amount of the curvature shortening δ:

$$F_{max} = n \frac{EA}{L} \delta = n \frac{\pi^2}{16} \frac{Eth}{L^2} \frac{g^2}{1 - \frac{c}{L}} \quad (8)$$

where n is the number of beams connected in parallel. The generated force can be scaled up by increasing the beam height h without consequence for the actuation voltage or by employing a large number of basic cells operating in parallel.

The maximum force of an actuator consisting of eight beam pairs (n=16) with the height h=5 µm, the width t=2 µm, the length L=200 µm, Young's modulus E=160 GPa and the curvature shortening δ=15.4 nm (see 3.2) is equal to F_{max}=1.97 mN.

4 FABRICATION

Successful implementation of the proposed actuator requires electrical isolation between mechanically joined beams. To achieve these requirements a SOI compatible trench isolation technology [8,9] is used. This technology employs trenches refilled with dielectric material to create, in a single layer, insulation and interconnection between released high-aspect-ratio microstructures (see Figure 2). The trench isolation process, initially developed for the fabrication of high-aspect-ratio inertial sensor [8], is extended by adding new design features while keeping the fabrication process virtually unchanged [9].

Basic fabrication steps are shown in Figure 1. The starting material for this two-mask process is a highly conductive (poly)silicon device layer on top of a sacrificial silicon oxide layer. Isolation trenches are etched in the device layer and subsequently refilled with a low stress silicon nitride. A maskless directional RIE process removes the silicon nitride layer from the top of the device layer. A second etching step defines mechanical structures. Deposition of a thin silicon nitride layer followed by a maskless RIE process results in a thin layer of silicon nitride on the sidewalls which is used to prevent short-circuiting between two parallel beams at the pull-in voltage. The final processing step is removing of the sacrificial oxide layer using a HF or BHF etch solution. This two mask fabrication process allows fabrication of released structures mechanically connected and electrically separated by a refilled isolation trench.

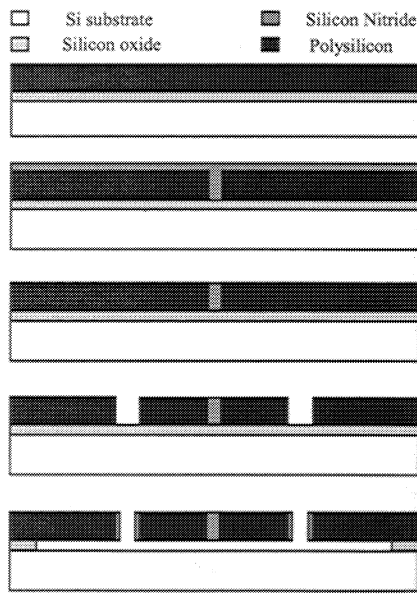

Figure 2: Fabrication process sequence

5 MEASUREMENTS

Test actuators have been fabricated using the trench isolation technology. A doped, 5 μm thick polysilicon layer on top of a 1 μm thick sacrificial silicon oxide layer was used as the starting material. The minimum thickness of the actuator beams t=2 μm was limited by the available photolithographic resolution. Isolation trenches, 2 μm wide, were refilled with a 1.2 μm thick LPCVD silicon nitride layer allowing electrical isolation and mechanical connection between neighboring beams (see Figure 3). The 100 nm thin LPCVD silicon nitride layer on sidewalls used to prevent short-circuiting between two beams at pull-in is also visible in this figure.

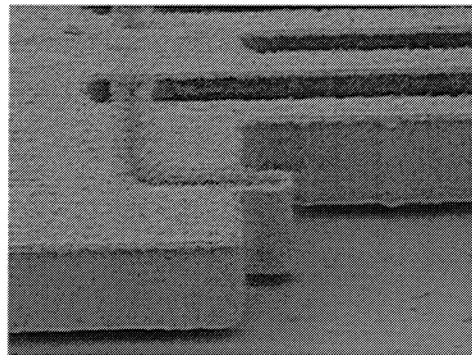

Figure 3: Trenches refilled with silicon nitride for electrical isolation between interconnected beams. Thin silicon nitride layer to prevent the shorting is visible on sidewalls.

The beam length L ranges between 200 μm and 300 μm and the mutual distance g between 2 μm to 3 μm. Actuators with a different number of beams n (4,8,16 and 32) are fabricated.

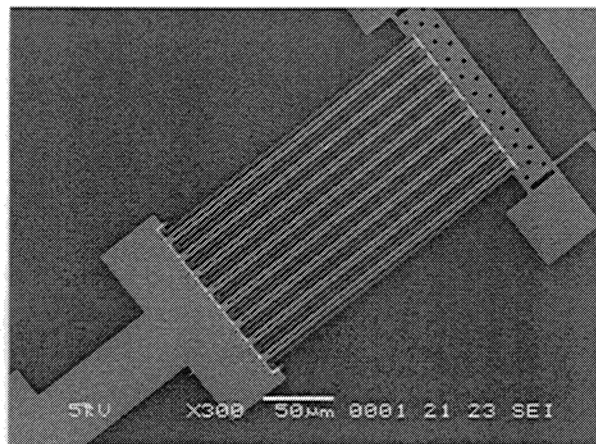

Figure 4: An actuator with 16 basic cells (32 parallel beams). Due to the charging during SEM session distinct electrical domain, including refilled trenches, are clearly visible.

Refilled isolation trenches are arranged in such a way to insure individual biasing of each beam in a basic cell (see Figure 4) despite an eventual mask misalignment.

Actuators are operated in the unstable regime, above the pull-in voltage allowing a contact between beams to occur (see Figure 5) in order to increase a longitudinal displacement δ (see Expression 7). A voltage higher than the pull-in voltage of an individual basic cell was applied to insure a simultaneously operation of all basic cells in an actuator. The simultaneously operation of 16 basic cells (32 beams) was registered. Actuators were operated with a harmonic voltage with amplitude from 30 V to 75 V depending on the beam length L and the mutual distance between beams g.

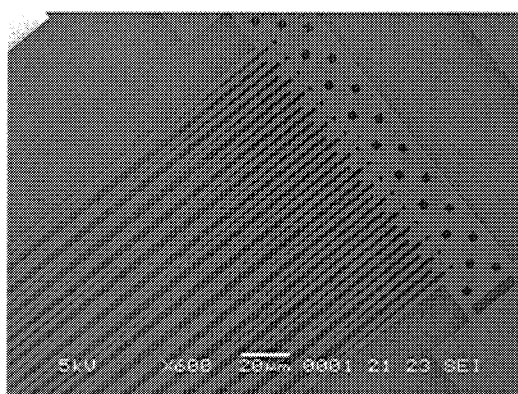

Figure 5: A SEM photograph of an actuator operated beyond the pull-in voltage. Parallel beams deflect simultaneously during operation.

A strain gauge with a mechanical amplifier (40x) was attached to a movable end of the actuator to measure under an optical microscope a longitudinal displacement. Springs with a known stiffness were used to suspend the movable actuator part in order to measure a generated force.

For an actuator containing 16 parallel beams, 2 μm wide, 200 μm long with 2 μm mutual distance between the beams, the maximum displacement of $\delta \approx 12$ nm and the maximum force $F_{max} \approx 1.5$ mN was measured. The active part of the actuator fits in a volume of 200 x 62 x 5 μm. To achieve a simultaneous operation of all actuator beams the higher actuation voltage (70 V) was applied then the pull-in voltage (57 V) measured for a single beam pair

6 CONCLUSIONS

An electrostatic microactuator suitable for low displacement applications is successfully fabricated and operated. The actuator uses a large number of basic units working in parallel and a built-in mechanical transformation to generate large force. Displacement and generated force of the fabricated actuators, operated at pull-in, are measured using integrated springs and strain meters. A large force (>1mN) with a controllable nanometer resolution step (<15 nm) was measured for a typical actuator containing 16 parallel beams 200 μm long, 2 μm wide, 5 μm high with 2 μm distance between. The actuator fits in a volume of 200 x 62 x 5 μm and is operated by the voltage of 70 V. Typical applications can include the contraction/elongation body of an inchworm motor, vibration excitation or friction measurements.

ACKWNOLEDGMENT

The authors would like to thank MESA+ Clean Room Staff for their assistance, A. Kooy and P. Linders from Deltamask for the mask processing, M. de Boer for many helpful discussions and M. Smithers for taking SEM photographs. This work is done within the 'A high capacity, low volume Scanning Probe Array Memory for application in embedded systems' project, funded by the Dutch Technology Foundation (STW).

REFERENCES

[1] D. Peichel, D. Marcus, R.N. Rizq, A.G. Erdman, W.P. Robins, D.L. Polla, Journal of Microelectromechanical Systems, Vol. 11, No. 2, Apr. 2002, pp.154-160.

[2] S. Konishi, K. Ohno, M. Munechika, Sensors and Actuators A, Vol. 97-98, No.1, Apr. 2002, pp.610-619.

[3] R. Yeh, S. Hollar, K.S.J. Pister, Journal of Microelectromechanical Systems, Vol. 11, No. 4, Aug. 2002, pp.330-336.

[4] N. Tas, J. Wissink, L. Sander, T. Lammerink, M. Elwenspoek, Sensors and Actuators A 70, 1998, pp.171-178.

[5] M.P. de Boer, J.M. Redmond, T.A. Michalske, SPIE proceeding v.3512, Materials and device characterzation in micromachining, Santa Clara, Sept. 1998, pp.241-250.

[6] P.M. Osterberg, R.K. Gupta, J.R. Gilbert, S.D. Senturia, Proc. Solid State Sensor and Actuator Workshop, Hilthon Head Island, SC, 1994, pp 184-188.

[7] J.M. Gere, S.P. Timoshenko, "Mechanics of materials", Chapman&Hall, 563-566, 1991.

[8] T.J. Brosnihan, J. M. Bustillo, A.P. Pisano and R.T. Howe, TRANSDUCERS '97, International Conference on Solid State Sensors and Actuators, Chicago, Jun.1997, pp.637-640.

[9] E. Sarajlic, E.Berenschot, G. Krijnen, M. Elwenspoek, Micro- and Nanoengineering Conference (MNE '02), Lugano, Switzerland, Sep. 2002.